Radiation Stability of Cations in Ionic Liquids. 3. Guanidinium Cations

ARTICLE *in* THE JOURNAL OF PHYSICAL CHEMISTRY B · OCTOBER 2013

Impact Factor: 3.3 · DOI: 10.1021/jp408253y · Source: PubMed

5 AUTHORS, INCLUDING:

Ilya Shkrob
Argonne National Laboratory
143 PUBLICATIONS **2,164** CITATIONS
SEE PROFILE

Timothy W Marin
Benedictine University
54 PUBLICATIONS **810** CITATIONS
SEE PROFILE

THE JOURNAL OF PHYSICAL CHEMISTRY B

Article

pubs.acs.org/JPCB

Radiation Stability of Cations in Ionic Liquids. 3. Guanidinium Cations

Ilya A. Shkrob,*[,†] Timothy W. Marin,[†,‡] Jason R. Bell,[§] Huimin Luo,[§] and Sheng Dai[∥]

[†]Chemical Sciences and Engineering Division, Argonne National Laboratory, 9700 South Cass Avenue, Argonne, Illinois 60439, United States

[‡]Chemistry Department, Benedictine University, 5700 College Road, Lisle, Illinois 60532, United States

[§]Energy and Transportation Science Division, Oak Ridge National Laboratory, Oak Ridge, Tennessee 37831, United States

[∥]Chemical Sciences Division, Oak Ridge National Laboratory, Oak Ridge, Tennessee 37831, United States

Supporting Information

ABSTRACT: Due to their superb structural versatility, guanidinium cations find increasing use as constituent ions in room temperature ionic liquids (ILs). This versatility allows fine-tuning of hydrophobicity, which is an important concern for the use of ILs as diluents for metal ion separations. However, the presence of six C−N bonds in such cations poses a question, whether the guanidinium based ILs can be considered as diluents for nuclear separations, given that the radiation emitted by the decaying radionuclides can break these relatively weak bonds over the use cycle of the solvent. As nothing is presently known about the radiolytic stability of the guanidinium cations, we addressed this question using 2-dialkylamino-1,3-dimethylimidazolidine based cations (R = Et, Pr, and Bu) as a representative model for the entire class of such cations, and assessed their stability in 2.5 MeV electron beam radiolysis. Electron paramagnetic resonance spectroscopy, nuclear magnetic resonance spectroscopy, and mass spectrometry have been used to establish chemical mechanisms for radiation damage in guanidinium cations. Our conclusion is that radiation stability of these cations is not significantly different from that of more familiar aliphatic and aromatic IL cations. In fact, these cations yield exceptionally stable radicals, and fragmentation occurs only in their radiolytically generated excited states. The predominant chemical pathway for the cation decomposition is the elimination of their aliphatic arms, with radiolytic yields of 0.65 to 1.06 to 1.46 per 100 eV from R = Et to R = Bu, respectively. The total loss of the parent cation was estimated as 2.62, 1.65, and 1.98 species per 100 eV. While this attrition is not negligible, it is comparable to other organic cations that have fewer fissile C−N bonds. Many of the products are either modified guanidinium ions or protonated bases that are not expected to interfere with radionuclide separations.

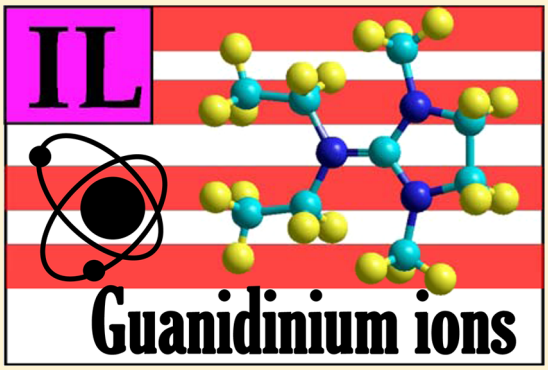

1. INTRODUCTION

Over the past decade, cyclic and acyclic guanidinium cations (Scheme 1) became species of choice in the synthesis of hydrophobic room temperature ionic liquids (ILs).[1−3]

Scheme 1. Structural Formulas for Tautomeric RRG5$^+$ Cations (C^+), the H Atom Loss Radicals ($C(-H)^{+\bullet}$), and Electron ($C^\bullet$) and H Atom Adducts ($CH^{+\bullet}$)

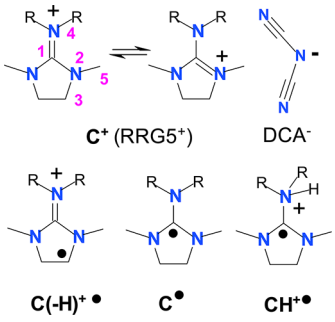

Derivatives of imidazolidine,[1] hexahydropyrimidine, tetrahydro-1,3,5-oxadiazine, triazoline,[3] and acyclical guanidinium cations[2,4−7] have been studied in ILs. The imidazolidine based cations with the structural formula given in Scheme 1 are among the easiest to synthesize, as the starting material is 1,3-dimethyl-2-imidazolidinone, a widely used aprotic polar solvent. ILs composed of the guanidinium cations have been used as organosynthetic catalysts,[7−9] solvents for SO_2 capture (see ref 6 and references therein),[10] high-energy materials,[3] and electrolytes for batteries[11,12] and photovoltaic cells.[2] The chief attraction of these guanidinium cations is the ease of tailoring their chemical structure using different substituting arms at the three nitrogen atoms, allowing fine-tuning of their properties. In contrast, many of the commonly used cations are derived from imidazolium, pyridinium, and other cations that have only one easily accessible substitution site, thereby offering less

Received: August 18, 2013
Revised: October 12, 2013
Published: October 22, 2013

freedom of structural variation.[3,5] Only onium cations (cyclical and acyclical ammonium, phosphonium, and sulfonium cations)[13−16] are comparable to these cations in structural versatility combined with the synthetic ease of preparation.

These properties make guanidinium based ILs an attractive choice for diluents in nuclear separations for "wet" spent fuel processing, as such separations depend on the balance of hydrophobicity for the constituent ions.[17] However, nothing is presently known about radiation stability of such guanidinium based ILs, whereas during the life cycle the diluent is exposed to 0.1−0.5 MGy of ionizing radiation.[18−24] Irradiation of the IL[25] is known to cause dissociation of carbon−heteroatom bonds (e.g., C−N bonds) in organic cations.[22,26−29] As the guanidinium cations have six such bonds (which is precisely what makes such cations attractive from a synthetic standpoint), the concern is that this high number of potentially fissile C−N bonds undermines their radiation stability as compared to other, more commonly used classes of organic cations. The question that we pursue in this study is whether the guanidinium cation based ILs are suitable for applications in strong radiation fields. Our conclusion is that the guanidinium cations do not exhibit rates of radiolytic decomposition that are significantly greater than those exhibited by other organic cations. This, in turn, paves way to their wider use in nuclear separations studies.

Radiation resistance of the guanidinium cations has been assessed using symmetrical (RRG5$^+$) imidazolidine based cations ($\mathbf{C}^+$) with two *n*-alkyl arms (R = Et, Pr, Bu) as a representative model for the entire class of such cations. Electron paramagnetic resonance (EPR) spectroscopy was used to observe radicals generated by 2.5 MeV electron beam irradiation of dicyanamide (DCA$^-$)[30] compounds, and electrospray ionization tandem mass spectrometry (ESI MS/MS) and nuclear magnetic resonance (NMR) were used to identify reaction products. The dicyanamide (DCA$^-$, Scheme 1) based ILs were chosen for scrutiny, as our previous research indicated superior radiation resistance of this anion to radiation.[31−35] To save space, many of the supporting tables, figures, details of synthetic and analytical protocols, and a list of abbreviations are placed in the Supporting Information. When referenced in the text, these materials have the designator "S", as in Figure 1S (Supporting Information).

2. EXPERIMENTAL AND COMPUTATIONAL METHODS

RRG5 DCA compounds were synthesized from the corresponding iodide compounds[1,3] by metathesis in aqueous Ag DCA solutions. Briefly, 1,3-dimethyl-2-imidazolidinone was refluxed with oxalyl chloride in anhydrous benzene to obtain 2-chloro-1,3-dimethylimidazolinium chloride (70% yield) that was subsequently reacted with an RNH_2 amine in CH_2Cl_2/NEt_3 to obtain 1,3-dimethyl-2-(1-R-imino)imidazolidine (RG5) that was purified by Kugelrohr distillation (~60% yield). This RG5 was quarternized by RI in the acentonitrile, and RRG5 I was obtained by evaporation of solvents. RRG5 I was then dissolved in deionized water and reacted with Ag DCA in order to obtain the corresponding ILs. The precipitate (AgI) was filtered. The aqueous phase was evaporated down, and the IL was lyophilized in a freeze-dryer. These RRG5 DCA compounds were 99.9+% pure by ESI MS and ^{1}H and ^{13}C NMR spectrometry. Hereafter, the atom numbering convention follows Scheme 1. Table 1S (Supporting Information) summarizes ^{1}H and ^{13}C NMR resonances with the chemical shifts given vs tetramethylsilane (TMS), and the mass spectra of the RRG5$^+$ cations are shown in Figure 1.

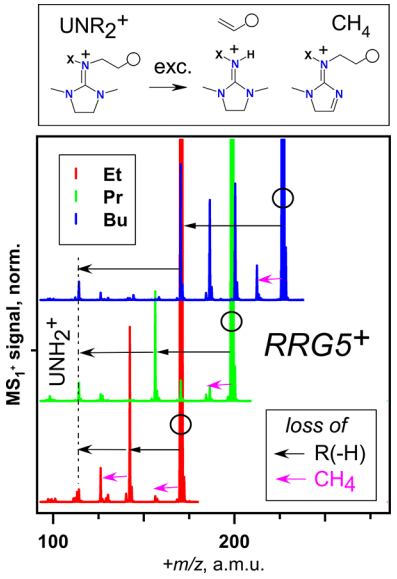

Figure 1. ESI MS_1^+ spectra of acetonitrile solutions of (unirradiated) RRG5 DCA. The open circles indicate the parent cation (UNR_2^+), and the arrows indicate R(−H) and methane loss. The dashed vertical line indicates the UNH_2^+ cation. The scheme above shows the two main fragmentation pathways in the gas phase cation.

The experimental and computational approaches were similar to those in parts 1 and 2 of this study.[34,35] For product analysis, the samples were evacuated and sealed in water-cooled borosilicate NMR tubes (O.D. 5 mm) and irradiated by 2.5 MeV electrons to a total dose of ~3.2 MGy using a dose rate of 6.8 kGy/s (1 Gy = 1 J/kg of the absorbed energy). ^{1}H and ^{13}C NMR spectra were obtained in dimethylsulfoxide-d_6 (DMSO-d_6), using an Avance DMX 500 MHz spectrometer (Bruker). ^{1}H−^{1}H COSY spectroscopy was used to establish proton connectivity. Tandem electrospray ionization mass spectra (ESI MS_n) were obtained using a Thermo Scientific LCQ Fleet ion trap mass spectrometer operating either in positive or negative modes ($MS_n^{\pm}$).[36] Liquid samples were injected directly in dilute acetonitrile solutions. $(\mathbf{CA})_n\mathbf{C}^+$ and $(\mathbf{CA})_n\mathbf{A}^-$ cluster ion series (n = 0−8) were detected (hereafter, $\mathbf{C}^+$ and $\mathbf{A}^-$ are the constituent ions). In section 3.2, only n = 0 ions of each series are reported. For analysis, radiolyzed samples were dissolved in acetonitrile to obtain 1−2 wt % solutions. High performance liquid chromatography−mass spectrometry (LCMS) was used to separate and identify isobaric products. To this end, a 2 μL aliquot was analyzed using reverse phase chromatography (ThermoScientific Accela suit) with ESI MS_1^+ detection (the same MS instrument). The phases and the elution conditions are summarized in Table 2S (Supporting Information).

For EPR spectroscopy, the samples were frozen by rapid immersion in liquid nitrogen and irradiated to 3 kGy at 77 K. The radicals were observed using a 9.44 GHz Bruker ESP300E spectrometer, with the sample placed in a flow helium cryostat (Oxford Instruments CF935). The magnetic field and the hyperfine coupling constants (hfcc's) are given in the units of Gauss (1 G = 10^{-4} T). If not stated otherwise, the first-derivative EPR spectra were obtained at 50 K using 2 G modulation at 100 kHz. The microwave power is indicated in the figures. The radiation-induced EPR signal from the E'_γ

dx.doi.org/10.1021/jp408253y | J. Phys. Chem. B 2013, 117, 14400−14407

center in the Suprasil sample tubes (that frequently overlapped with the resonance lines of organic radicals) is shadowed white in the EPR spectra. The calculations of the hfcc's and radical structures were carried out using a density functional theory (DFT) method with the B3LYP functional[37,38] and 6-31+G(d,p) basis set from Gaussian 03.[39] In the following, a_{iso} denotes the isotropic hfcc corresponding to the hfc tensor and **B** denotes the anisotropic part. Powder EPR spectra were simulated using first-order perturbation theory assuming isotropic **g**-tensors.

3. RESULTS AND DISCUSSION

3.1. Theoretical Considerations and EPR Spectroscopy. In radiolysis, autoionization of highly excited states of cations ($\mathbf{C}^+$) and anions ($\mathbf{A}^-$) in IL solvent causes electron detachment from these ions.[26,27,40] In Na DCA,[31,33] *oxidized* pseudohalide anion yields a dimer radical anion ($\mathbf{A}_2^{-\bullet}$) with a N−N $\sigma^2\sigma^{1*}$ bond between the unique nitrogens,[32] which is the product of addition of the imidyl radical (oxidized anion, $\mathbf{A}^\bullet$) to the parent anion. In the previously studied DCA compounds, including ILs, no products of anion *reduction* were observed.[31,32]

In radiolysis, an organic cation can be either oxidized or reduced. Onium cations with aliphatic arms cannot be reduced,[31] but guanidinium cations (due to the presence of the $C_1{=}N_{2,4}$ double bonds shown in Scheme 1) are good electron acceptors. In the gas phase, the adiabatic electron affinity for $MeMeG5^+$ is estimated as 3.76 eV (Table 3S, Supporting Information), which is comparable to that of 1,2-dimethylimidazolium (3.94 eV).[35] The resulting electron adduct (radical $\mathbf{C}^\bullet$, Scheme 1) is a σ-radical with the unpaired electron density on trigonal carbon-1 (Figure 1S, structure ii, and Tables 4S and 5S, Supporting Information). For cations derived from aromatic heterocycles, such $\mathbf{C}^\bullet$ radicals can form $\sigma^2\sigma^{1*}$ bonds (5-membered rings)[32,35] or π-sandwich dimers (6-membered rings)[34] with their parent cations, but our DFT calculations suggest that the electron adducts of guanidinium are too sterically congested to form these radical cations (Figure 1S, structure iii, and Table 3S, Supporting Information), so the corresponding reaction is endergonic by 2.43 eV. This is in contrast to $^\bullet C(CN)_3$ radicals generated by oxidation of tricyanomethanide anion ($C(CN)_3^-$) that readily form $C_2(CN)_6^{-\bullet}$ radical anions in the corresponding ILs.[33]

Cation oxidation typically yields hydrogen atom loss radicals like the $\mathbf{C}(-H)^{+\bullet}$ radical shown in Scheme 1, as the radical dications promptly deprotonate (C_1-N_4 dissociation with the elimination of $NEt_2^{+\bullet}$ is also possible, section 3.2). For $RRG5^+$, the intermediate $\mathbf{C}^{2+\bullet}$ dication can deprotonate from carbon-3, carbon-5 sites, and also from the aliphatic arms. Our DFT calculations indicate that the energies of the corresponding C−H bonds are within 100 meV of each other; the C_3-H_3 bonds are the weakest (Table 3S, Supporting Information). Using the computed hfcc tensors (Tables 4S and 5S, Supporting Information), we simulated the corresponding first-derivative EPR spectra of these radicals in Figure 2S (Supporting Information). The EPR spectrum of the $\mathbf{C}^\bullet$ radical is sensitive to the extent of trigonality in carbon-1 (Table 5S, Supporting Information) that depends on the imposed symmetry; as different conformers are close in energy (<250 meV), matrix effects can be significant. The EPR spectra for $\mathbf{C}(-H)^{+\bullet}$ radicals centered at different carbon atoms are quite different, as seen from the EPR simulations in Figure 2S (Supporting Information).

Figure 2 exhibits the experimental EPR spectra obtained for irradiated RRG5 DCA compounds at 50 K. These EPR spectra

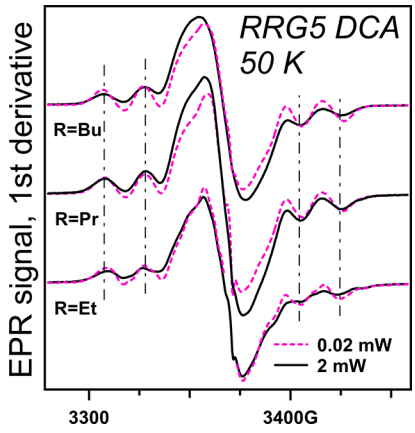

Figure 2. First-derivative EPR spectrum of irradiated frozen RRG5 DCA observed at 50 K (obtained at 0.02 and 0.2 mW, 2.5 MeV electron beam radiolysis at 77 K). The vertical lines indicate the outer resonance lines of the $\mathbf{C}(-H)^{+\bullet}$ radical shown in Scheme 1.

indicate the presence of at least two progenitor radicals, one of which is responsible for the resonance lines indicated with vertical lines and the other is responsible for the unresolved singlet resonance line at the center of the plot. In Figure 3a, we juxtapose low-power EPR spectra for three RRG5 DCA compounds (R = Et, Pr, and Bu). These EPR spectra are almost identical, which excludes the C_α-centered $\mathbf{C}(-H)^{+\bullet}$ radicals, as these radicals would have different numbers of β-protons for $EtEtG5^+$ vs the two other cations. For the same reason, the interior radicals can also be excluded, whereas the

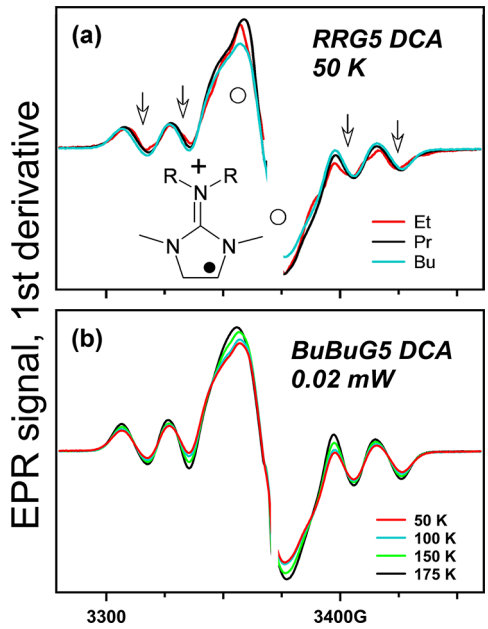

Figure 3. (a) Comparison of normalized low-power (0.02 mW) EPR spectra from Figure 2. (b) Normalized EPR spectra for irradiated BuBuG5 DCA as a function of temperature. The arrows in panel a indicate the resonance lines of the $\mathbf{C}(-H)^{+\bullet}$ radical, and the open circles indicate the singlet line of the $\mathbf{C}^\bullet$ radical.

dx.doi.org/10.1021/jp408253y | J. Phys. Chem. B 2013, 117, 14400−14407

terminal radicals would have EPR spectra inconsistent with the features indicated by the arrows in Figure 3a. As the $\mathbf{C}(-H)^{+\bullet}$ radical centered on carbon-5 is a triplet (Figure 2S, Supporting Information), it can be excluded too. By exclusion and similarity to the simulated EPR spectrum in Figure 2S (Supporting Information), the likely progenitor of these features is the carbon-3 centered H loss radical shown in Scheme 1 and Figure 1S, structure iv (Supporting Information). Apparently, radiolytic oxidation of the $RRG5^+$ cations causes deprotonation from exclusively carbon-3 sites in the imidazolidine ring.

The unresolved singlet is clearly from the electron adduct shown in Figure 1S, structure ii (Supporting Information), as its envelope corresponds to the broadened EPR spectra shown in the simulations in Figure 2S (Supporting Information). In support of this attribution, there is an approximate parity in the yields of the $\mathbf{C}^\bullet$ and $\mathbf{C}(-H)^{+\bullet}$ radicals, as suggested by double integration of their respective contributions. As the yields of oxidation and reduction are always the same, this parity would be expected if the dicyanamide anion is not oxidized or reduced. Indeed, neither the corresponding imidyl radical ($\mathbf{A}^\bullet$) nor the dimer radical anion ($\mathbf{A}_2^{-\bullet}$) are observed, suggesting that radiolytic ionization of the $RRG5^+$ cations is more facile than that of the DCA^- anions. An alternative explanation is that the imidyl radicals ($\mathbf{A}^\bullet$) generated by oxidation of DCA^- (which is a *pseudohalide* anion) abstract H from cations more rapidly than they form N_1-N_1 bonds with the parent anions (which has been observed in some *halide* ILs).[41,42]

To our knowledge, the $\mathbf{C}^\bullet$ radical of the suggested type has never been observed previously, although the intermediate triaminomethyl radicals were postulated to occur in the gas phase, where this radical dissociates to NH_3 and $HNC^\bullet NH_2$.[43,44] The analogous reaction for the electron adduct of $RRG5^+$ would be the elimination of $NMeR_2$ with the formation of radical **1** shown in Figure 3S (Supporting Information). According to our DFT calculation, for $MeMeG5^+$, this reaction would be endergonic by 1.56 eV, so this fragmentation is unlikely (also, there is no evidence for radical **1** in our EPR spectra, see Figure 3S (Supporting Information) for simulations). Our EPR results also exclude the formation of radicals generated through $C_1{=}N_4$ bond scission and H atom adducts ($CH^{+\bullet}$ radicals) to N_2 and/or N_4 atoms (Scheme 1S and Figure 3S, Supporting Information). These latter were commonly found in radiolytic reduction of aromatic cations[26,27,34,35] where these species are formed via protonation of the electron adducts. The estimated gas-phase proton affinity of the $\mathbf{C}^\bullet$ radicals of the $MeMeG5^+$ cations is about 1 eV lower than that for 2,3-dimethylimidazolium (Table 3S, Supporting Information, and ref 35), suggesting that this protonation does not occur.

Figure 3b shows the temperature dependence of normalized EPR spectra for BuBuG5 DCA. It is seen that both of the radicals persist to 175 K, suggesting their relatively high stability in this matrix. For EtEtG5 DCA (Figure 4S, Supporting Information), we observed the preferential decay of the $\mathbf{C}^\bullet$ radical, but still both $\mathbf{C}(-H)^{+\bullet}$ and $\mathbf{C}^\bullet$ radicals were present in the irradiated sample warmed to 215 K. Warming of the sample to 300 K selectively removed the contribution from the $\mathbf{C}^\bullet$ radicals, and the resulting EPR spectrum closely resembled the simulated EPR spectrum for H loss radical at carbon-3, further validating our attribution. The remarkable stability of this $\mathbf{C}(-H)^{+\bullet}$ radical results from inhibition of recombination through steric hindrance. As other such secondary radicals, in addition to recombination, this $\mathbf{C}(-H)^{+\bullet}$ radical can be expected to disproportionate, yielding the $C_3{=}C_{3'}$ double bond cation shown in Figure 1S, structure vii (Supporting Information). The corresponding H_2 loss ions were observed in the mass spectra (Figure 4).

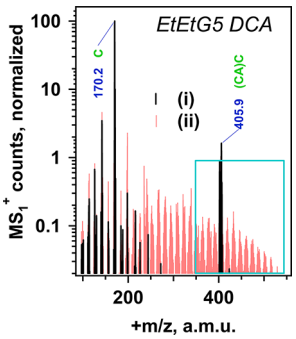

Figure 4. ESI MS_1^+ spectrum of acetonitrile solutions of RRG5 DCA, before (i) and after (ii) irradiation to 3.23 MGy. Note the logarithmic vertical scale. The square indicates $(\mathbf{CA})C'^+$ cluster cations. The mass peaks and their attributions are indicated in Figure 5S in the Supporting Information.

We conclude that the guanidinium cations are resistant to fragmentation in their oxidized and reduced forms. The resulting radicals are exceptionally stable. There is no evidence for radical formation in the aliphatic arms (R−) of these $RRG5^+$ cations, which is uncommon: for cations that we studied previously, the loss of hydrogen from the aliphatic arms was facile.[26,27,31,35,41] The import of these observations is that cation fragmentation can occur only in electronically excited states.

3.2. Mass Spectrometry Analyses. Previous studies indicate that organic cations of BR^+ type, where B is the base and R is the aliphatic arm, undergo carbon-heteroatom cleavage from their excited states, releasing the corresponding 1-olefin ($R(-H)$) and the protonated base (BH^+)

$$\{BR^+\}^{**} \rightarrow BH^+ + R(-H) \qquad (1)$$

In the following, we introduce the notation U for the imidazolidine ring, so the parent cations are represented as UNR_2^+ (Figure 1). Our DFT calculations indicate that reaction 1 for $UNEt_2^+$ is endergonic by 0.63 eV, and for the resulting $UNHEt^+$ cation, it is endergonic by 0.8 eV (Scheme 1S, Supporting Information). Both of these reactions are observed in the ESI MS_1^+ spectra of $RRG5^+$ cations shown in Figure 1: the most abundant secondary cation is the $UNHR^+$ followed by the UNH_2^+. The $UH^{+\bullet}$ species are also observed, (Table 6S, Supporting Information), suggesting the dissociation of the C_1-N_4 bond, which (according to our DFT calculations) requires excitation >5 eV in these guanidinium cations. The elimination of one or two CH_4 molecules from these UNR_2^+ and $UNHR^+$ cations is also observed, whereas collisional excitation of these same cations resulted only in R(−H) elimination. As this methane elimination occurs regardless of the substitution at nitrogen-4, it appears that the eliminated group is N_2-Me, suggesting that the electronically excited cation yields the $U(-CH_4)NR_2^+$ species shown in Figure 1 (see also Figure 1S, structure ix, Supporting Information). According to our calculations, for $UNMe_2^+$, the loss of the first and the second CH_4 molecule is exergonic by 0.43 and 1.38 eV, respectively (Scheme 1S, Supporting Information); i.e., thermodynamically this reaction is more favorable than reaction

dx.doi.org/10.1021/jp408253y | J. Phys. Chem. B 2013, 117, 14400−14407

1. In addition to such C−N dissociation reactions, there is also stepwise loss of methylene units from the aliphatic arm −R (Figure 1 and Table 6S, Supporting Information), suggesting the occurrence of C−C bond scission that is concurrent with the C−N scissions. These observations point to the ease of C−N and C−C bond fragmentation in the excited guanidinium cations.

In Figures 4 and 5S (Supporting Information), we compare MS_1^+ spectra of EtEtG5 DCA before and after 2.5 MeV electron radiolysis (3.23 MGy). As seen from the plot, the yield of the product cations is quite low, but there are many of such products, and there is a dense copse of mass peaks every 13−14 amu stretching over to m/z +500. Comparisons with LCMS results (Table 7S, Supporting Information) suggest that cations with m/z > 350 amu are mainly (**CA**)C′$^+$ cluster ions, where C′$^+$ is a fragment cation. Some of the lower mass peaks belong to the fragments of higher mass cations (as seen in Figure 1). We used LCMS to establish that the corresponding peaks are indeed the mass ions of the corresponding products.

The yields of the fragment ions derived of the parent cation, before and after irradiation, are comparable except for $UNMeEt^+$ (methylene loss) and $UNHEt^+$ and UNH_2^+ (single and double R(−H) loss). There is also a prominent $U(-H_2)NMe_2$ peak, but the yield was difficult to quantify due to the mass overlap. The products with the highest yield are those corresponding to the R(−H) loss and R-arm attachment to the parent cation (with radiolytic yields of 0.67 and 0.42 per 100 eV, respectively), suggesting that reaction 1 is the main fragmentation pathway in radiolysis (this is seconded by NMR spectroscopy, as shown in section 3.3). Other species (that are also present in radiolysis of $PrPrG5^+$ and $BuBuG5^+$, Figures 6S and 7S, Supporting Information) include **C**−Alk^+ cations that are obtained by either single or multiple alkyl substitution, **C**−NR_2^+ and **C**−$N(CN)_2^+$ cations, **C**−$U(-Me)^+$ adducts (Schemes 1 and 2S, Supporting Information) and related products, and **C**−**C**$^+$ cations. The latter cations may be the products of recombination of **C**$(-H)^{+\bullet}$ and **C**$^\bullet$ radicals.

The presence of the $-NR_2$ and −U(Me) substituted products suggests the occurrence of C_1-N_4 bond dissociation or elimination of groups from the **C**−**C**$^+$ adducts. The prominence of the **C**−Alk−$U(-Me)^+$ series is noteworthy, as there are several isomer structures that can be involved (Scheme 2S, Supporting Information) depending on the specific sites for the loss and the gain of −Me and −Alk groups in the parent cation. We view these products as specifically −U(Me) derivatives using the guidance of ^{13}C NMR spectroscopy, as discussed below. The presence of the species containing −U(Me) bases is also suggested by the strong retention of the corresponding protonated forms on the cation-exchange columns and the ease of their elution on neutral columns in LCMS analysis (Table 7S, Supporting Information).

While the general fragmentation patterns are similar for all three $RRG5^+$ cations, a major difference emerges in the loss of the parent cation, which are estimated to be 2.62, 1.65, and 1.98 species per 100 eV for the Et-, Pr-, and Bu-derivatives, respectively. The smaller size of the $EtEtG5^+$ cation appears to be detrimental, as the excitation causes a higher yield of C−N fragmentation in the ring. In $BuBuG5^+$, there is excessive C−N and C−C fragmentation in the aliphatic chains, and $PrPrG5^+$ provides the optimum regarding minimization of fragmentation; actually, it is one of the more stable organic cations.[35] These decomposition rates are not significantly different from such rates for other organic cations (see parts 1 and 2).[34,35]

3.3. NMR Analyses. As a first step in the NMR analyses, ^1H and ^{13}C chemical shifts for a large selection of cation and neutral structures were calculated using DFT theory (Figures 8S and 9S, Supporting Information, respectively). Our interpretation of NMR spectra rests on the insights obtained from these calculations.

^1H NMR spectra of irradiated $RRG5^+$ DCA are remarkably similar: many of the resonances with proton shifts between 4 and 9 ppm are reproduced through the series (Figure 5a and 10S, Supporting Information), and there are groups of resonances with chemical shifts between 2 and 4 ppm that are also reproduced (Figures 5b and 6 and Figures 11S−13S, Supporting Information).

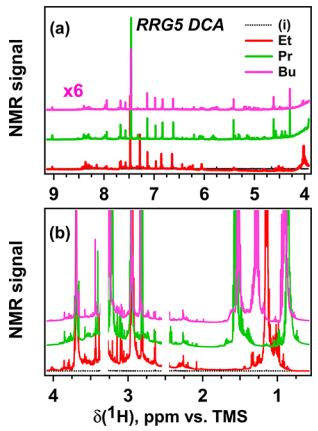

Figure 5. Comparison of normalized ^1H NMR spectra of irradiated RRG5 DCA compounds. Trace (i) is the NMR spectrum of the DMSO-d_6 solvent. The screened parts of the spectra contain the resonance lines of the solvent impurity. Note the 6-fold expansion of the vertical scale in panel a vs panel b (the resonance lines are attributed in Figure 10S in the Supporting Information).

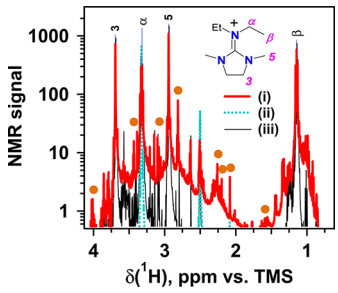

Figure 6. Trace i: ^1H NMR spectrum (0.5−4 ppm region) of irradiated EtEtG5 DCA (3.23 Gy). Traces (iii) and (iii) are the spectra of the solvent (DMSO-d_6) and unirradiated EtEtG5 DCA. Note the logarithmic vertical scale. The filled circles indicate the proton resonance lines of the products that are conserved across the RRG5 DCA series. The resonance lines are annotated in Figure 11S in the Supporting Information.

The most prominent product features in Figures 5b and 6 are the resonances with chemical shifts of 2.80, 3.26, 3.40, and 7.45 ppm. Table 8S (Supporting Information) summarizes coupling patterns and $J(^1H-^1H)$ constants for protons (where we were able to determine these), Table 9S (Supporting Information) lists COSY cross peaks observed in the two-dimensional NMR

dx.doi.org/10.1021/jp408253y | J. Phys. Chem. B 2013, 117, 14400−14407

experiments, and some of the groups of the coupled protons are pictorially represented in Figure 14S (Supporting Information). Figures 15S and 16S (Supporting Information) show the corresponding ^{13}C NMR spectra. The product resonances occur in two regions: 0−70 ppm (Figure 15S, Supporting Information) and 110−170 ppm (Figure 16S, Supporting Information). There are almost no resonance lines upfield of carbon-1 in the parent RRG5$^+$ cation, and there are reproducible lines at 160, 158, 157.8, 131−133, 123, and 120 ppm.

The only two structures that are expected to yield ^{13}C shifts upfield of carbon-1 in the parent cation are U(—2CH$_4$)NXY$^+$ (in carbons-1 and 3) and U(—Me)NXY$^+$ (in carbon-3, see Figure 8S, Supporting Information). It appears that the yield of such structures (observed as minor products in the MS$_1^+$ spectra, Tables 6S and 7S, Supporting Information) must be low. The 120−123 ppm peaks belong to carbons at the double C═C bonds in the U(—H$_2$)NXY$^+$ cations or their neutral counterparts (Figures 8S and 9S, Supporting Information). These charged species would account for the ^1H resonance lines with chemical shifts around 7.5 ppm, and their neutral forms would account for the ^1H resonance lines at 5.5−6 ppm. Some of the peaks downfield of the cyanide carbons are likely to belong to the terminal and penultimate carbons in C═C groups in the aliphatic chains. The existence of such groups is also suggested by observations of protons with chemical shifts at 5−6.5 ppm with cross peaks in the expected range (Table 9S, Supporting Information) and large *J*-couplings (>10 Hz, Table 8S, Supporting Information). The elimination of R(—H) olefins is consistent with these observations: for EtEtG5$^+$, there is a resonance line at 124 ppm (corresponding to ethylene), for PrPrG5$^+$ there are lines for the terminal and penultimate carbons at 116.5 and 133 ppm, respectively (propylene), and for BuBuG5$^+$ there are lines at 113.5 and 140.5 ppm (1-butene).

Some of the 131−133 ppm resonances can be from carbon-1 nuclei in neutral U═C< units (Scheme 8S, Supporting Information) or even UNR molecules (that is, deprotonated UNHR$^+$ cations). The N$_2$═C$_3$—H protons in charged ═U(—CH$_4$) and —U(—Me) groups would account for 9 and 8.5 ppm resonances, respectively. The low yield of such species is suggestive of the general preference for reaction 1, which is supported by the mass spectra given in section 3.2. The upfield shifted resonances for α-protons originate from —N(H)R groups of the cations, which is consistent with their correlation patterns (Table 9S and Figure 14S, Supporting Information). The 2.83−2.90 ppm resonances for N$_2$—Me protons downfield of the same lines in the parent cation are likely to belong to the UNHR$^+$ species (Figures 6 and 11S, Supporting Information), as they correlate with the 8.35 ppm resonance that is typical of the >C═N$^+$HR cations in DMSO-d_6 (Table 9S, Supporting Information). The latter resonance exhibits the expected *dt* coupling pattern with a large $J(^1H—^{14}N)$ constant of ∼46.7 Hz.[45] We attribute 158 ppm resonances to carbon-1 nuclei in these cations. The yield of this UNHR$^+$ species systematically increases in the irradiated RRG5 DCA from 0.65 to 1.06 to 1.46 per 100 eV from R═Et to R═Bu (whereas, in Table 6S, Supporting Information, the same yields were estimated as 0.67, 0.3, and 0.25 per 100 eV, respectively). This inconsistency results in the ease of the secondary fragmentation, as evidenced by the mass spectra, underlying the difficulties of obtaining accurate and unbiased estimates using this method. We believe that NMR, as a more direct method, yields more reliable estimates.

The 145−150 ppm resonances are consistent with the further loss of the aliphatic groups in the UNH$_2^+$ and U(−H$_2$)NH$_2^+$ cations; the presence of neutral −U(Me) groups (Figure 9S, Supporting Information, and Scheme 2S, Supporting Information) is another possibility (which is also consistent with the MS$_1^+$ spectra, see above). The yield of such species is only ∼10% of the predominant product, which is the UNHR$^+$ cation. All in all, ∼8.2% of the protons (for EtEtG5 DCA and PrPrG5 DCA) and 14% of the protons for BuBuG5 DCA became dispersed across the ^1H NMR spectrum at a dose of ∼3.2 MGy (not counting the resonance lines masked by the resonance lines in the parent compound).

4. CONCLUDING REMARKS

While the cyclic guanidinium cations shown in Scheme 1 are superbly resistant to radiation induced oxidation and reduction, these cations are much less resistant to fragmentation in their excited state(s), in which multiple C−C and C−N bond dissociation occurs. The predominant dissociation pathway is reaction 1, which results in the loss of aliphatic arms, but there is also elimination of the methyl groups. The resulting bases are capable of metal ion binding unless protonated in acidic solution. For the latter reason, the guanidinium based ILs may not be suitable for nuclear extractions (forward or back) at low acidity.

The most remarkable observations about these guanidinium cations, from a mechanistic standpoint, is that they do not appear to be more unstable radiolytically as compared to other IL cations, despite the presence of the multiple fissile C−N bonds. Given the exceptional structural versatility of such cations,[19,22,28,34,35] our study indicates that guanidinium based IL can and should be considered as candidates for IL based nuclear separations, with a special awareness of low-yield generation of bases that need to remain protonated during their entire use cycle.

■ ASSOCIATED CONTENT

Ⓢ Supporting Information

A PDF file containing a list of abbreviations, Schemes 1S and 2S, Tables 1S−9S, and Figures 1S−16S with captions, including radical geometries, experimental and simulated EPR spectra, and NMR spectra. This material is available free of charge via the Internet at http://pubs.acs.org.

■ AUTHOR INFORMATION

Corresponding Author

*E-mail shkrob@anl.gov. Phone: (630) 252-9516.

Notes

The authors declare no competing financial interest.

■ ACKNOWLEDGMENTS

We thank S. Chemerisov, R. Lowers, D. Quigley, S. Lopykinski, and J. Muntean for technical support. The work at Argonne and Oak Ridge was supported by the US-DOE Office of Science, Division of Chemical Sciences, Geosciences and Biosciences under Contract Nos. DE-AC02-06CH11357 and DE-AC05-0096OR22725, respectively. Programmatic support via a DOE SISGR grant "An Integrated Basic Research Program for Advanced Nuclear Energy Separations Systems Based on Ionic Liquids" is gratefully acknowledged.

REFERENCES

(1) Xie, H.; Zhang, S.; Duan, H. An Ionic Liquid Based on a Cyclic Guanidinium Cation Is an Efficient Medium for the Selective Oxidation of Benzyl Alcohols. *Tetrahedron Lett.* **2004**, *45*, 2013−2015.

(2) Wang, P.; Zakeeruddin, S. M.; Graetzel, M.; Kantlehner, W.; Mezger, J.; Stoyanov, E. V.; Scherr, O. Novel Room Temperature Ionic Liquids of Hexaalkyl Substituted Guanidinium Salts for Dye-Sensitized Solar Cells. *Appl. Phys. A: Mater. Sci. Process.* **2004**, *79*, 73−77.

(3) Gao, Y.; Arritt, S. W.; Twamley, B.; Shreeve, J. M. Guanidinium-Based Ionic Liquids. *Inorg. Chem.* **2005**, *44*, 1704−1712.

(4) Kulkarni, P. S.; Branco, L. C.; Crespo, J. G.; Nunes, M. C.; Raymundo, A.; Afonso, C. A. M. Comparison of Physicochemical Properties of New Ionic Liquids Based on Imidazolium, Quaternary Ammonium, and Guanidinium Cations. *Chem.—Eur. J.* **2007**, *2007*, 8478−8488.

(5) Bogdanov, M. G.; Petkova, D.; Hristeva, S.; Svinyarov, I.; Kantlehnerb, W. New Guanidinium-Based Room-Temperature Ionic Liquids. Substituent and Anion Effect on Density and Solubility in Water. *Z. Naturforsch.* **2010**, *65b*, 37−48.

(6) Yu, G.; Chen, X. SO_2 Capture by Guanidinium-Based Ionic Liquids: A Theoretical Study. *J. Phys. Chem. B* **2010**, *115*, 3466−3477.

(7) Rad-Moghadam, K.; Youseftabar-Miri, L. Tetramethylguanidinium Triflate: An Efficient Catalyst Solvent for the Convergent Synthesis of Fused Spiro[1,4-Dihydropyridine-Oxindole] Compounds. *J. Fluorine Chem.* **2012**, *135*, 213−219.

(8) Li, S.; Lin, Y.; Xie, H.; Zhang, S.; Xu, J. Brønsted Guanidine Acid-Base Ionic Liquids: Novel Reaction Media for the Palladium-Catalyzed Heck Reaction. *Org. Lett.* **2006**, *8*, 391−394.

(9) Wang, W.; Shao, L.; Cheng, W.; Yang, J.; He, M. Brønsted Acidic Ionic Liquids as Novel Catalysts for Prins Reaction. *Catal. Commun.* **2008**, *9*, 337−341.

(10) Huang, J.; Riisager, A.; Wasserscheid, P.; Fehrmann, R. Reversible Physical Absorption of SO_2 by Ionic Liquids. *Chem. Commun.* **2006**, 4027−4029.

(11) Fang, S.; L., Y.; J., W.; Zhang, H.; K., T.; Kamijima, K. Guanidinium-Based Ionic Liquids as New Electrolytes for Lithium Battery. *J. Power Sources* **2009**, *191*, 619−622.

(12) Zhang, X. Y.; H., F. S.; X., Z. Z.; Yang, L. Li/$LiFePO_4$ Battery Performance with a Guanidinium-Based Ionic Liquid as the Electrolyte. *Chin. Sci. Bull.* **2011**, *56*, 2906−2910.

(13) Welton, T. Room-Temperature Ionic Liquids. Solvents for Synthesis and Catalysis. *Chem. Rev.* **1999**, *99*, 2071−2083.

(14) Hallett, J. P.; Welton, T. Room-Temperature Ionic Liquids: Solvents for Synthesis and Catalysis. 2. *Chem. Rev.* **2011**, *111*, 3508−3576.

(15) Plechkova, N. V.; Seddon, K. R. Applications of Ionic Liquids in the Chemical Industry. *Chem. Soc. Rev.* **2008**, *37*, 123−150.

(16) Smiglak, M.; Metlen, A.; Rogers, R. D. The Second Evolution of Ionic Liquids: From Solvents and Separations to Advanced Materials - Energetic Examples from the Ionic Liquid Cookbook. *Acc. Chem. Res.* **2007**, 1182−1192.

(17) Sun, X. Q.; Luo, H. M.; Dai, S. Ionic Liquids-Based Extraction: A Promising Strategy for the Advanced Nuclear Fuel Cycle. *Chem. Rev.* **2012**, *112*, 2100−2128.

(18) Yuan, L. Y.; Peng, J.; Xu, L.; Zhai, M. L.; Li, J. Q.; Wei, G. S. Influence of Gamma-Radiation on the Ionic Liquid [C(4)mim][PF_6] During Extraction of Strontium Ions. *Dalton Trans.* **2008**, 6358−6360.

(19) Bosse, E.; Berthon, L.; Zorz, N.; Monget, J.; Berthon, C.; Bisel, I.; Legand, S.; Moisy, P. Stability of [$MeBu_3N$][Tf_2N] under Gamma Irradiation. *Dalton Trans.* **2008**, 924−931.

(20) Tarabek, P.; Shengyan, L.; Haygarth, K.; Bartels, D. M. Hydrogen Gas Yields in Irradiated Room-Temperature Ionic Liquids. *Radiat. Phys. Chem.* **2009**, *78*, 168−172.

(21) Wishart, J. F.; Shkrob, I. A. *The Radiation Chemistry of Ionic Liquids and Its Implications for Their Use in Nuclear Fuel Processing*; American Chemical Society: Washington, DC, 2009; pp 119−134.

(22) Le Rouzo, G.; Lamouroux, C.; Dauvois, V.; Dannoux, A.; Legand, S.; Durand, D.; Moisy, P.; G., M. Anion Effect on Radiochemical Stability of Room-Temperature Ionic Liquids under Gamma Irradiation. *Dalton Trans.* **2009**, 6175−6184.

(23) Berthon, L.; Chabronnel, M.-C. Radiolysis of Solvents Used in Nuclear Fuel Reprocessing. In *Ion Exchange and Solvent Extraction, A Series of Advances*; Moyer, B. A., Ed.; CRC Press: Boca Raton, FL, 2010; Vol. *19*, pp 429−513.

(24) Dhiman, S. B.; Goff, G. S.; Runde, W.; LaVerne, J. A. Hydrogen Production in Aromatic and Aliphatic Ionic Liquids. *J. Phys. Chem. B* **2013**, *117*, 6782−6788.

(25) Wishart, J. F. Ionic Liquid Radiation Chemistry. In *Ionic Liquids: Coiled for Action*; Seddon, K. R., Rogers, R. D., Eds.; Wiley, Ltd.: Chichester, U.K., 2013; in press.

(26) Shkrob, I. A.; Marin, T. W.; Chemerisov, S. D.; Hatcher, J. L.; Wishart, J. F. Radiation Induced Redox Reactions and Fragmentation of Constituent Ions in Ionic Liquids. 2. Imidazolium Cations. *J. Phys. Chem. B* **2011**, *115*, 3889−3902.

(27) Shkrob, I. A.; Wishart, J. F. Free Radical Chemistry in Room-Temperature Ionic Liquids. In *Encyclopedia of Radicals in Chemistry, Biology and Materials*; Chatgilialoglu, C., Studer, A., Eds.; John Wiley & Sons, Ltd.: Chichester, U.K., 2012; pp 433−448.

(28) Berthon, L.; Nikitenko, S. I.; Bisel, I.; Berthon, C.; Faucon, M.; Saucerotte, B.; Zorz, N.; Moisy, P. Influence of Gamma Irradiation on Hydrophobic Room-Temperature Ionic Liquids [BuMeIm] PF_6 and [BuMeIm]$(CF_3SO_2)_2N$. *Dalton Trans.* **2006**, 2526−2534.

(29) Wishart, J. F. Ionic Liquids and Ionizing Radiation: Reactivity of Highly Energetic Species. *J. Phys. Chem. Lett.* **2010**, *1*, 3225−3231.

(30) MacFarlane, D. R.; Forsyth, S. A.; Golding, J.; Deacon, G. B. Ionic Liquids Based on Imidazolium, Ammonium and Pyrrolidinium Salts of the Dicyanamide Anion. *Green Chem.* **2002**, *4*, 444−448.

(31) Shkrob, I. A.; Chemerisov, S. D.; Wishart, J. F. The Initial Stages of Radiation Damage in Ionic Liquids and Ionic Liquid-Based Extraction Systems. *J. Phys. Chem. B* **2007**, *111*, 11786−11793.

(32) Shkrob, I. A.; Wishart, J. F. Charge Trapping in Imidazolium Ionic Liquids. *J. Phys. Chem. B* **2009**, *113*, 5582−5592.

(33) Shkrob, I. A.; Marin, T. W.; Wishart, J. F. Ionic Liquids Based on Polynitrile Anions: Hydrophobicity, Low Proton Affinity, and High Radiolytic Resistance Combined. *J. Phys. Chem. B* **2013**, *117*, 7084−7094.

(34) Shkrob, I. A.; Marin, T. W.; Wishart, J. F. Radiation Stability of Cations in Ionic Liquids. 2. Improved Radiation Resistance through Charge Delocalization in 1-Benzylpyridinium. *J. Phys. Chem. B* **2013**, DOI: 10.1021/jp408242b.

(35) Shkrob, I. A.; Marin, T. W.; Luo, H.; Dai, S. Radiation Stability of Cations in Ionic Liquids. 1. Alkyl and Benzyl Derivatives of 5-Membered Ring Heterocycles. *J. Phys. Chem. B* **2013**, DOI: 10.1021/jp4082432.

(36) MS_1 corresponds to the first quadrupole and MS_2 corresponds to collision induced dissociation (of mass selected ions) modes of operation.

(37) Becke, A. D. Density-Functional Exchange-Energy Approximation with Correct Asymptotic Behavior. *Phys. Rev. A* **1988**, *38*, 3098−3100.

(38) Lee, C.; Yang, W.; Parr, R. G. Development of the Colle-Salvetti Correlation-Energy Formula into a Functional of the Electron Density. *Phys. Rev. B* **1988**, *37*, 785−789.

(39) Frisch, M. J.; Trucks, G. W.; Schlegel, H. B.; Scuseria, G. E.; Robb, M. A.; Cheeseman, V. G.; Montgomery, J. A., Jr.; Vreven, K. N.; Kudin, J. C.; Burant, J. C. *Gaussian 03*, rev. C.02; Gaussian, Inc.: Wallingford, CT, 2004.

(40) Shkrob, I. A.; Marin, T. W.; Chemerisov, S. D.; Wishart, J. F. Radiation and Radical Chemistry of NO_3^-, HNO_3, and Dialkylphosphoric Acids in Room-Temperature Ionic Liquids. *J. Phys. Chem. B* **2011**, *115*, 10927−10942.

(41) Shkrob, I. A.; Marin, T. W.; Chemerisov, S. D.; Wishart, J. F. Radiation-Induced Redox Reactions and Fragmentation of Constituent Ions in Ionic Liquids. I. Anions. *J. Phys. Chem. B* **2011**, *115*, 3872−3888.

(42) Shkrob, I. A.; Marin, T. W.; Crowell, R. A.; Wishart, J. F. Photo- and Radiation- Chemistry of Halide Anions in Ionic Liquids. *J. Phys. Chem. A* **2013**, *117*, 5742−5756.
(43) Shaffer, S. A.; Turecek, F.; Cerny, R. L. The (Dimethylamino)-Methyl Radical. A Neutralization-Reionization and Ab Initio Study. *J. Am. Chem. Soc.* **1993**, *115*, 12117−12124.
(44) Hao, C.; Seymour, J. L.; Turecek, F. Electron Super-Rich Radicals in the Gas Phase. A Neutralization-Reionization Mass Spectrometric and Ab Initio/RRKM Study of Diaminohydroxymethyl and Triaminomethyl Radicals. *J. Phys. Chem. A* **2007**, *111*, 8829−8843.
(45) Olah, G. A.; Burrichter, A.; Rasul, G.; Hachoumy, M.; Prakash, G. K. S. 1h, 13c, 15n Nmr and Ab Initio/IGLO/GIAO-MP2 Study of Mono-, Di-, Tri-, and Tetraprotonated Guanidine. *J. Am. Chem. Soc.* **1997**, *119*, 12929−12933.